PHYSICSAccess Research Paper
ISSN Online: 2756-3898, ISSN Print: 2714-500X https://doi.org/10.47514/phyaccess.sp.iss.2022.1.006

Investigating the Performance of Perovskite Solar Cells Using Nickel Oxide and Copper Iodide as P-type Inorganic layers by SCAPS-1D Simulation

Olayinka M Jimoh[1], Ikechiamaka N Florence[1], Akinsanmi Akinbolati[1], Chima Nnachi[2], Clement Ajani[3], Philibus M Gyuk[4], Suleiman Magaji[5] and Eli Danladi[6]

[1] Department of Physics, Federal University Dutsin-Ma, Katsina State, Nigeria
[2] Department of Chemistry, Federal University Dutsin-Ma, Katsina State, Nigeria
[3] Academy of Contemporary Food Engineering, South China University of Technology, Guangzhou, China
[4] Department of Physics, Kaduna State University, Kaduna, Kaduna State, Nigeria
[5] Department of Electronics and Communications, Nigerian Defence Academy, Kaduna, Kaduna State, Nigeria
[6] Department of Physics, Federal University of Health Sciences, Otukpo, Benue State, Nigeria

Corresponding E-mail: yinka4jimoh@gmail.com

Received 28-11-2022
Accepted for publication 16-12-2022
Published 28-12-2022

Abstract

Lead-based perovskite solar cells (PSCs) have drawn much research attention over the years due to their impressive light-to-power conversion efficiency (PCE), low temperature with easy manufacturing, tolerance to defects, high absorption coefficient and low cost. In this paper, the effect of absorber thickness, absorber band gap, absorber doping concentration, and electron transport material (ETM) thickness of PSC with two inorganic hole transport materials (HTM) was investigated using one-dimensional solar capacitance simulation (SCAPS-1D) software. Results obtained indicates that solar cell containing CuI as HTM performed better than that with NiO. A power conversion efficiency of 16.65%, fill factor (FF) of 82.43%, current density (J_{sc}) of 24.83 mA/cm^2 and voltage (V_{oc}) of 0.83 V were obtained for CuI with an enhancement of 1.15 times in PCE, 1.10 in J_{sc} and 1.17 in FF over the initial device and PCE of 15.74%, FF of 74.69 %, J_{sc} of 27.22 mA/cm^2 and V_{oc} of 0.77 V for NiO with an enhancement of 1.20 times in PCE, 1.25 times in J_{sc} and 1.15 in FF when compared with the initial device. The result therefore, shows that CuI as HTM performed better than NiO and implies that critical selection of the absorber parameters is a very key factor to enhance solar cell devices.

Keywords: Perovskite solar cell; HTM; Optimization; SCAPS.

I. INTRODUCTION

Hybrid organic-inorganic perovskite solar cells (PSCs) have generated a great deal of interest in recent years as a means of creating clean, renewable energy, and a series of amazing developments have been documented [1-6]. These perovskite materials possess a number of outstanding qualities, including a tunable band gap, a high light extinction coefficient, a long carrier diffusion length and high carrier mobility, a high carrier mobility and defect tolerance, as well as ease of manufacturing using a low temperature process [7-8]. Additionally, when compared to current prospective

photovoltaic (PV) technologies, perovskite solar modules offer a rapid energy payback time with a gain that exceeds that of the best organic material-based devices [9]. Currently, PSCs have large power conversion efficiency (PCE) greater than 25% [10-12].

However, ZnO-based PSC has gained a lot of attention recently because of its abundance in nature, ease of manufacturing, low cost, and high electron mobility compared to other devices [13, 14]. Effective PSCs with good PCE use doped spiro-OMeTAD HTMs [15]. Additionally, extra dopants must be added to spiro-OMeTAD to improve its hole-transporting property due to its very limited hole mobility; its synthesis procedure is very tedious as such its replacement with inorganic HTM is desirable, this is because, inorganic HTM have greater mobility, cheap production costs, and outstanding stability [16]. For optimization, it's essential to have a good understanding of how each layer in PSCs architecture affects the devices' performance.

In this work, a computer simulation program has been used to compare the consequences of substituting organic component (spiro-OMeTAD) with two alternative inorganic minerals, NiO and CuI. The valence bands of the HTL and the perovskite layer are aligned differently as a result of the various band gap energies (E_g) and electron affinities of these semiconductor materials. The inorganic compounds, NiO and CuI used in this work are seen to be good candidates for use as electron-blocking layer and holes transport substances [17].

II. SIMULATION

With the help of the one-dimensional code SCAPS-1D, numerical simulations of perovskite solar cells utilizing the planar structure were carried out. The Poisson and continuity equations for holes and electrons under steady-state conditions are the three fundamental semiconductor equations that this simulation tool numerically solves [11].

The hetero junction solar cells are simulated in this study using three input layers: low p-type doped perovskite ($CH_3NH_3PbI_3$) is used as the active layer, and n-type transparent conducting oxide, ZnO is employed as the ETL and P-type NiO and CuI are used independently to compare their performance as HTL. Therefore, the effect of absorber bandgap, doping concentration, defect density, and absorber thickness on the performance of the solar cell were analyzed.

Electron and hole thermal velocities are $1 \times 10^7\ cm/$s. To estimate the current-voltage (J-V) characteristics, all simulations are performed under light of $1000\ W/m^2$, temperature of $300\ K$, and an air mass of 1.5 air mass. Tables I and II provide an overview of the device and material parameters values used in SCAPS-1D simulation and taken from theories and literatures.

Table I Simulation parameters of PSCs devices [18-24]

Parameters	FTO	ETM(ZnO)	Absorber	HTMs CuI	NiO)
Thickness (μm)	0.4	0.055	0.45	0.05	0.05
Band gap energy E_g (eV)	3.5	3.3	1.55	3.4	3.8
Electron affinity χ (eV)	4.0	4.0	3.90	2.1	1.4
Relative permittivity ε_r	9	9.0	6.50	10.0	10.7
Effective conduction band density Nc (cm^{-3})	2.2×10^{18}	3.7×10^{21}	2.2×10^{18}	2.5×10^{18}	2×10^{19}
Effective valance band density Nv (cm^{-3})	2.2×10^{18}	1.8×10^{19}	2.2×10^{18}	1.8×10^{19}	1.8×10^{19}
Electron mobility μ_n ($cm^2\ V^{-1}\ s^{-1}$)	20	100	2	$2\times\ 10^4$	12.0
Hole mobility μ_p ($cm^2\ V^{-1}\ s^{-1}$)	10	25	2	2×10^4	28.0
Donor concentration N_D (cm^{-3})	1×10^{19}	1×10^{18}	0	0	0
Acceptor concentration N_A (cm^{-3})	0	0	1×10^{13}	1×10^{20}	1×10^{20}
Defect density N_t (cm^{-3})	1×10^{15}	1×10^{13}	2.5×10^{13}	1×10^{14}	1×10^{14}

Table II Absorber and interface defect parameters [18-24]

Parameters	$CH_3NH_3PbI_3$	ZnO/$CH_3NH_3PbI_3$ interface	$CH_3NH_3PbI_3$/(CuI/NiO) interface
Defect type	Neutral	Neutral	Neutral
Capture cross section for electrons (cm^2)	2×10^{-15}	2×10^{-16}	2×10^{-15}
Capture cross section for holes (cm^2)	2×10^{-15}	2×10^{-16}	2×10^{-15}
Energetic distribution	Gaussian	Single	Single
Energy level with respect to E_v (eV)	0.500	0.650	0.650
Characteristic energy (eV)	0.1	0.1	0.1
Total density (cm^{-3})	1×10^{15}–1×10^{19}	1×10^{18}	1×10^{18}

III. Results and Discussion

A. Energy level diagram of the PSC

Fig. 1(b), which depict the valance and conduction band offset at the ZnO/$CH_3NH_3PbI_3$ interface with values of 0.13 eV and 1.82 eV, respectively, reveal the structure of the band diagram. In order to prevent recombination with electrons in the perovskite, these values favor the flows of holes to the metal-back contact, as opposed to $CH_3NH_3PbI_3$/CuI, which favors the electron to the front electrode at 1.80 eV and 0.16eV, respectively. When using Nickel Oxide as HTM, the band offset is seen in Fig. 1a with values for the interfaces ZnO/$CH_3NH_3PbI_3$ of 0.26 eV and 1.80 eV and $CH_3NH_3PbI_3$/NiO of 2.45 eV and 0.20 eV, respectively.

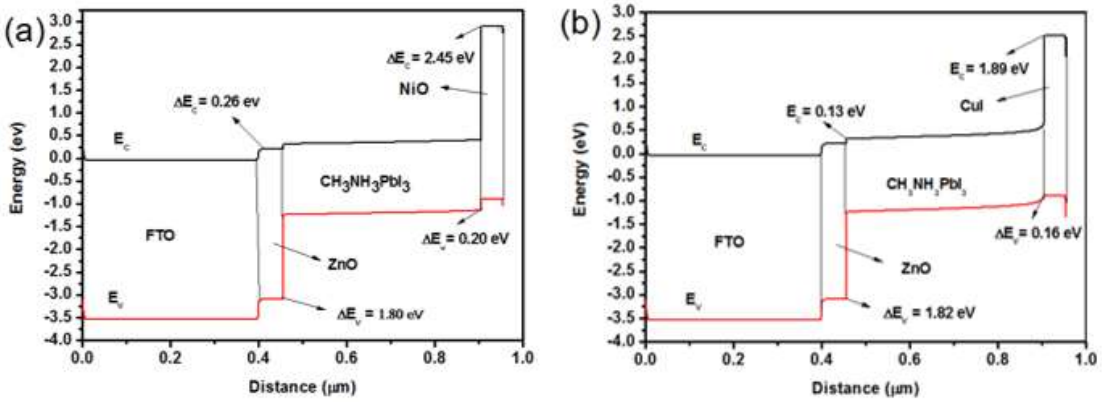

Fig. 1 (a) Energy band diagram of ZnO/$CH_3NH_3PbI_3$/CuI and (b) Energy band diagram of ZnO/$CH_3NH_3PbI_3$/NiO

B. Performance study of the initial simulation

The current density–voltage curve under illumination has been plotted with these initial parameters as shown in Fig. 2a.

When NiO is used as the HTM, the short-circuit current density (J_{sc}) is 21.76 mA/cm^2, the open-circuit voltage (V_{oc}) is 0.9290 V, the fill factor (FF) is 64.77%, and the power conversion efficiency (PCE) is 13.09 %. However, when CuI is used as the HTM, the short-circuit current density (J_{sc}) is 22.06 mA/cm^2, open-circuit voltage (V_{oc}) of 0.9272 V, Fill Factor (FF) of 70.53%, and PCE of 14.43%.The simulated device's performance agrees with lead-based PSCs' experimental findings [25].

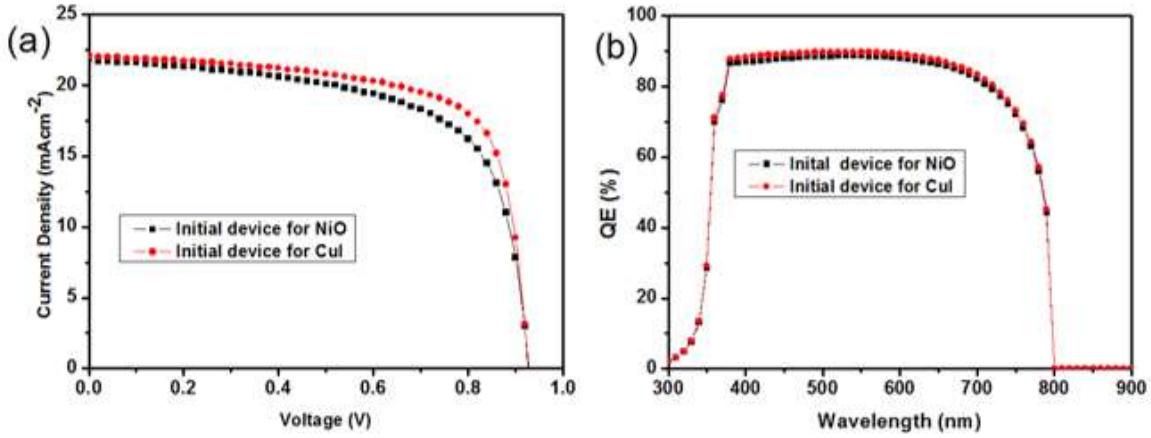

Fig. 2 (a) *J-V* curves of PSC with initial parameter, (b) quantum efficiency (QE) of the device with initial device.

This uniformity demonstrates that the input settings are appropriate and almost accurate to the device. The plot Fig. 2b has an incident photon-to-current efficiency (IPCE) that is within the range of 300 and 900 nm with a maximum of 90% at 550 nm. In $CH_3NH_3PbI_3$, the optical absorption border is red shifted to 800 nm, which translates to a band gap of 1.55 eV [26].

C. Effect of Absorber Thickness

One of the key factors affecting the overall performance of the solar cell is the thickness of the absorber layer.

Simulations have been run for both CuI and NiO HTM-based device in the thickness range of 0.1 to 0.6 μm to confirm the ideal absorber thickness. The other variables remained constant. The simulated results for NiO and CuI demonstrate that when the absorber layer thickness increases, the J_{sc} and V_{oc} also rise because more photons will be absorbed by a thicker layer, which will result in the formation of more electron-hole pairs. But as the charges travel a greater distance for diffusion, the likelihood of recombination likewise rises with a larger absorber layer. The PCE increases as thickness also increase up to 0.45 μm for NiO and 0.40 μm for CuI and then decreases due to less photons generated from the absorber. There was a decay in fill factor (FF) for both HTMs due to effect of electric field in the absorber [27]. Hence the optimized thickness of the absorber layer is 0.40 μm for CuI based and 0.45 μm for NiO based device. At this thickness the maximum PCE of NiO is 13.09% and $J_{sc} = 21.75\ mA/cm^2$, $V_{oc} = 0.92\ V$, $FF = 64.77\%$ and PCE of CuI based HTM device is 14.43% and $Jsc = 22.06\ mA/cm^2$, V_{oc}=0.92 V, FF=22.07%. The correlation of all the devices with various parameters are as shown in Fig. 4 (a-h). Table III shows the metric parameters dependency of the device with the absorber thickness.

The *J-V* and quantum efficiency curves are shown in Fig. 3(a) and (b).

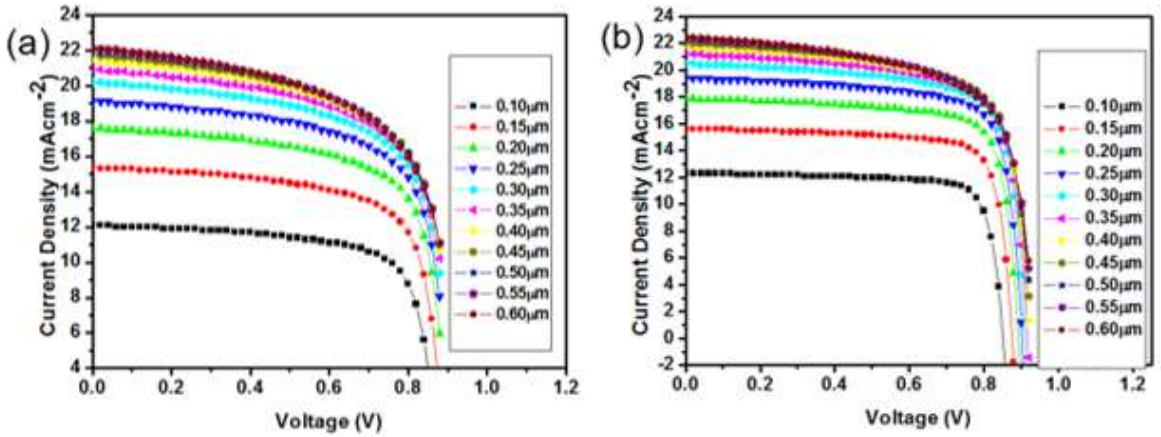

Fig. 3(a) J-V curves of PSC with varied absorber thickness for NiO and (b) J-V curves of PSC with varied absorber thickness for CuI-based HTM device

Table III Dependence of solar cell performance on the thickness of Absorber

Parameters (T μm)	V_{oc} (V) NiO	V_{oc} (V) CuI	J_{sc} (mA/cm^2) NiO	J_{sc} (mA/cm^2) CuI	FF (%) NiO	FF (%) CuI	PCE (%) NiO	PCE (%) CuI
0.10	0.87	0.85	12.09	12.30	72.24	80.30	7.58	8.42
0.15	0.89	0.88	15.36	15.62	71.05	79.95	9.68	10.84
0.20	0.90	0.89	17.59	17.87	69.90	77.95	11.07	12.42
0.25	0.91	0.90	19.19	19.42	68.81	76.38	11.96	13.38
0.30	0.92	0.91	20.18	20.48	67.75	74.95	12.52	13.98
0.35	0.93	0.92	20.91	21.22	66.72	73.46	12.86	14.30
0.40	0.93	0.92	21.42	21.73	65.73	71.98	13.03	14.43
0.45	0.93	0.93	21.76	22.07	64.77	70.53	13.09	14.43
0.50	0.93	0.93	21.98	22.29	63.83	69.12	13.08	14.35
0.55	0.94	0.94	22.12	22.43	62.91	67.78	13.01	14.21
0.60	0.94	0.94	22.19	22.50	62.01	66.53	12.89	14.03

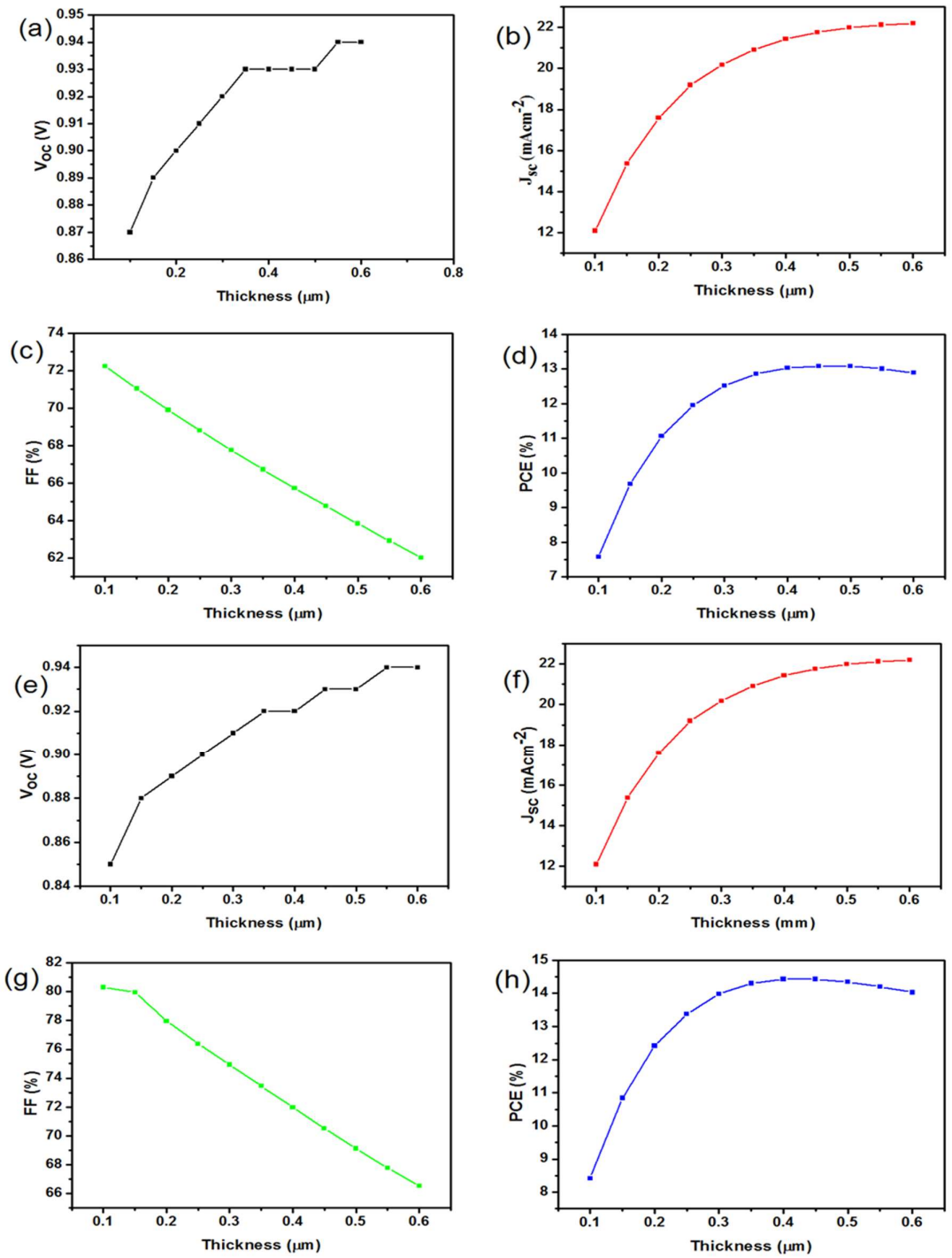

Fig. 4(a-d) variation in solar cell parameters with increase in absorber layer thickness of NiO and (e-h) for CuI

D. Influence of Bandgap on absorber layer

Band gap is the distance between the valence band of electrons and the conduction band. Essentially it represents the minimum amount of energy needed to free an electron from its bond, and this energy differs from among semiconductor materials. Fig. 5a-d shows the *J-V* and Q-E plots for the NiO

and CuI based PSC with respect to varied bandgap. From Table IV as the bandgap values increases, the value of the V_{oc} also increases but J_{sc} decrease while FF increases. The PCE values increase with increase in bandgap until it reaches its optimum values and then start decreasing because J_{sc} is a function of recombination, current and as value of recombination current increase, the value of J_{sc} tends to decrease thereby reducing the performance of the device. As the value of the bandgap increases, the exciton binding energy decreases, so the electron and holes can spill to generate photo current with little sunlight. At an optimum value of absorber, the value of bandgap increases to 1.40 eV when using NiO as HTM with PCE of 14.18%, V_{oc} of 0.78 V, J_{sc} value of 26.59 mA/cm^2 and FF of 68.09%, and at 1.5 eV for CuI as HTM, the PCE value was 14.54%, J_{sc} is 23.63 mA/cm^2 , V_{oc} is 0.88 V and FF is also found to be 69.95%. The device metric parameters with a correlation of the bandgap are shown in Fig. 6 (a-h).

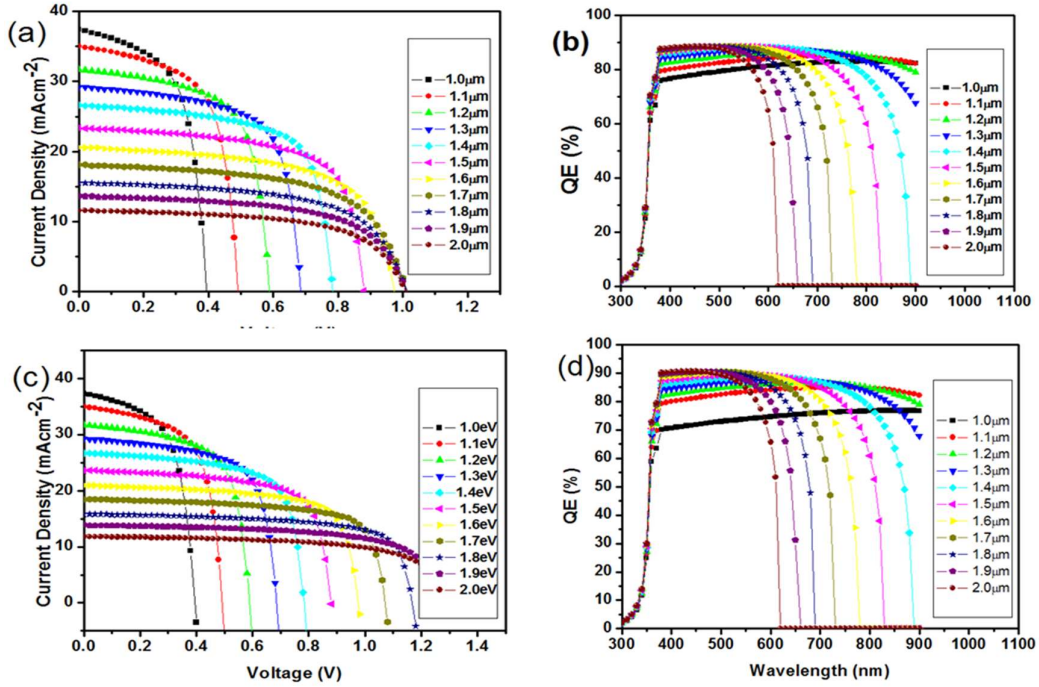

Fig. 5 (a) *J-V* curves of PSC with varied band gap of absorber for NiO, (b) Quantum efficiency vs. wavelength of PSC with varied band gap of absorber for NiO, (c) *J-V* curves of PSC with varied band gap of absorber for CuI and (d) Quantum efficiency vs. wavelength of PSC with varied band gap of absorber for CuI

Table IV Dependence of solar cell performance on the band gap of Absorber

E_g (eV)	V_{oc} (V) NiO	V_{oc} (V) CuI	J_{sc} (mAcm^{-2}) NiO	J_{sc}(mAcm^{-2}), CuI	FF (%) NiO	FF (%) CuI	PCE (%) NiO	PCE (%) CuI
1.0	0.395	0.395	37.372	37.401	60.210	59.760	8.89	8.82
1.1	0.493	0.493	34.977	34.981	62.900	62.890	10.83	10.83
1.2	0.589	0.589	31.720	31.733	65.230	65.250	12.19	12.19
1.3	0.686	0.683	29.220	29.262	66.940	67.040	13.42	13.46
1.4	0.783	0.783	26.588	26.721	68.090	68.730	14.18	14.39
1.5	0.880	0.880	23.372	23.633	66.920	69.950	13.77	14.54
1.6	0.975	0.976	20.560	20.902	62.250	71.120	12.48	14.50
1.7	1.014	1.072	18.087	18.432	60.080	71.640	11.02	14.15
1.8	1.015	1.168	15.527	15.826	60.160	70.22	9.48	12.98
1.9	1.013		13.601	13.860	60.470		8.33	11.59
2.0	1.011		11.594	11.810	60.740		7.12	9.90

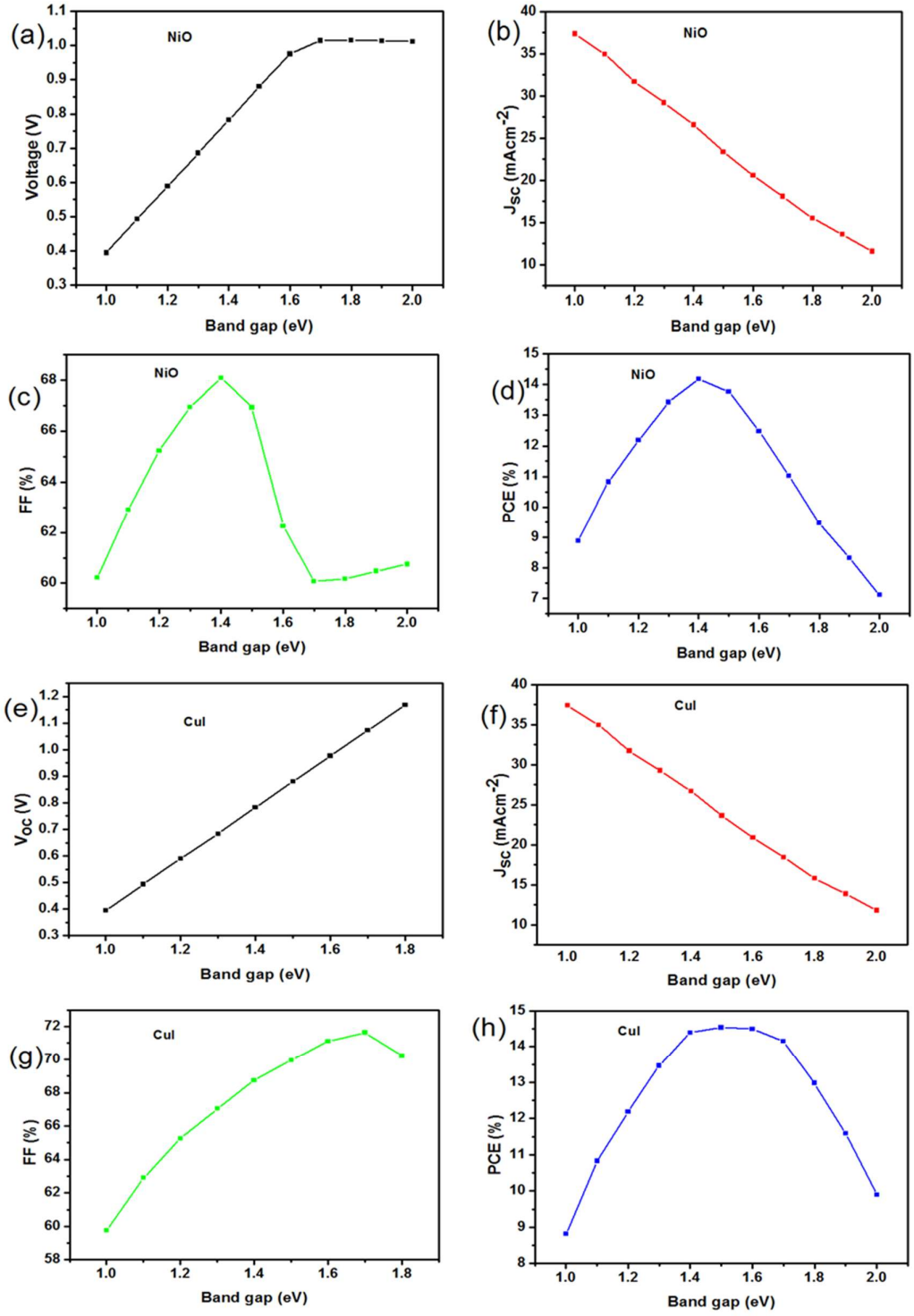

Fig. 6 (a-d): Variation in solar cell parameters with increasing bandgap of absorber for NiO and (e-h) for CuI

E. Influence of doping concentration on absorber layer

The electrical behavior of the layers in a solar cell is determined by the doping of a photoactive material, which has an impact on the device's performance. It contributes significantly to the enhancement of semiconductor device properties, including photovoltaic [28]. An appropriate dopant can be added to the absorber layer to enhance PSC performance. Impurities in the absorber layer need to be improve slightly due to lead perovskite's instability in air and moisture. By selecting N_A values for both HTM that fall between the ranges of 10^{10} and 10^{18} cm^{-3} the impact of doping concentration on the performance of perovskite solar cells is taken into consideration. While other variables were held constant, the dopant concentrations of perovskite were changed from 10^{10} - 10^{18} cm^{-3} in order to observe their impact on solar cell performances.

With the doping concentration of perovskite increasing from 10^{10} - 10^{18} cm^{-3} in external quantum efficiency (QE) greatly improves (see Fig. 7), which suggests that the generation rate of the photogenerated carriers increases under the same incident photon number.

Therefore, improving the photo-absorption efficiency and the J_{sc} requires an appropriate doping concentration of the perovskite absorption layer. There was no any significant effect on the solar cell performance parameter at dopant concentration 10^{10} - 10^{13} cm^{13} for both HTM because of the generation of recombination that cancel the new charges but however, the Voc drops quickly when the N_A exceeds 10^{15} cm^{-3}. From the standpoint of the built-in electric field, which is strengthened with the increase in doping concentration, the variation in the performance of the cell with the doping concentration may be explained. The improvement of the electric field encourages the separation of carriers, which leads to an improvement in the functionality of the cell. However, further boosting the doping level will result in a larger Auger recombination rate, which is not good for raising V_{oc}. To achieve the highest performance with NiO, a concentration of 10^{15} cm^{-3} is ideal, whereas CuI necessitates a concentration of 10^{16} cm^{-3}. In Fig. 8, these values are depicted as correlation of the thickness with metric parameters. These parameters were attained at the ideal values: CuI had a V_{oc} of 0.87 V, J_{sc} of 23.08 mA/cm^2, FF of 82.54%, and PCE of 16.59 % while NiO had a Voc of 0.91 V, J_{sc} of 22.08 mA/cm^2, FF of 71.66%, and PCE of 14.38%. Table V shows the various photovoltaic performance with varied doping concentration.

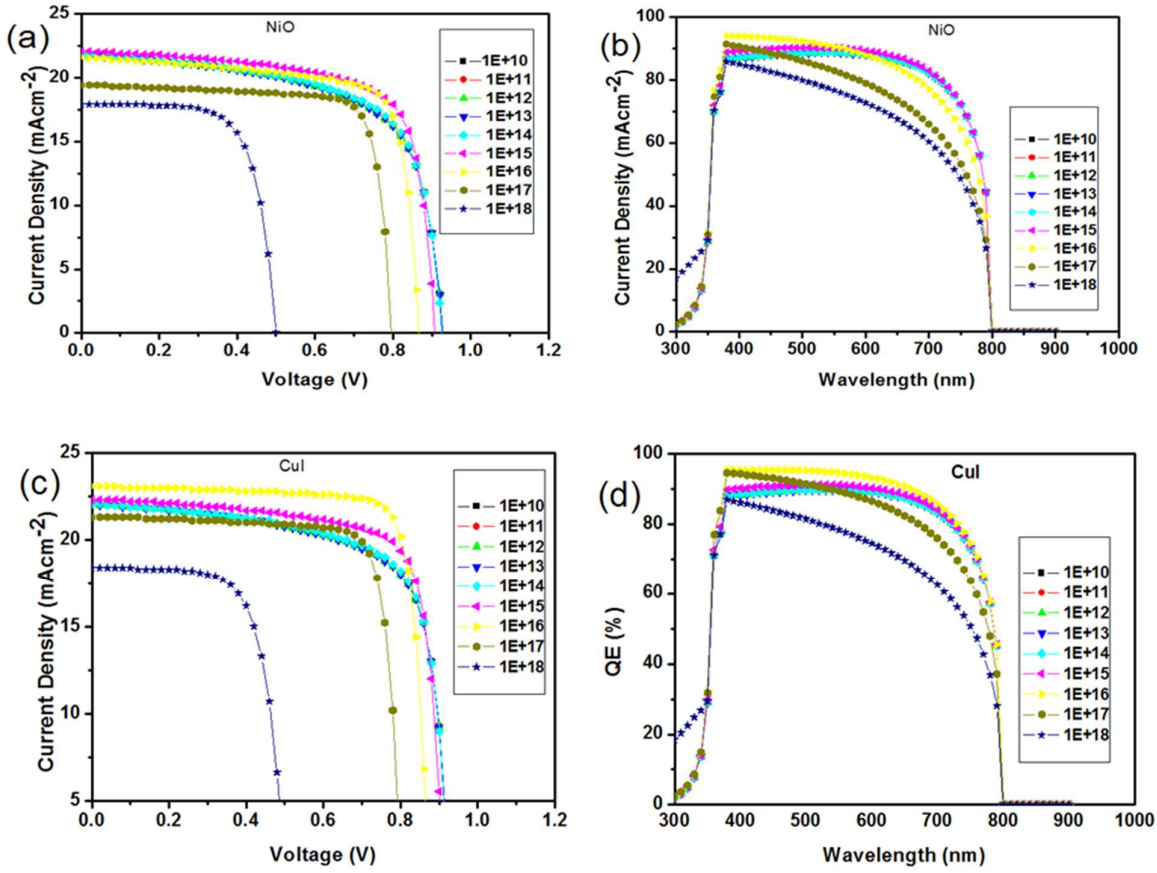

Fig. 7(a) - (b): *J-V* curves of PSC and QE with different values of doping concentration (N_A) on absorber layer for NiO and (c)-(d) for CuI

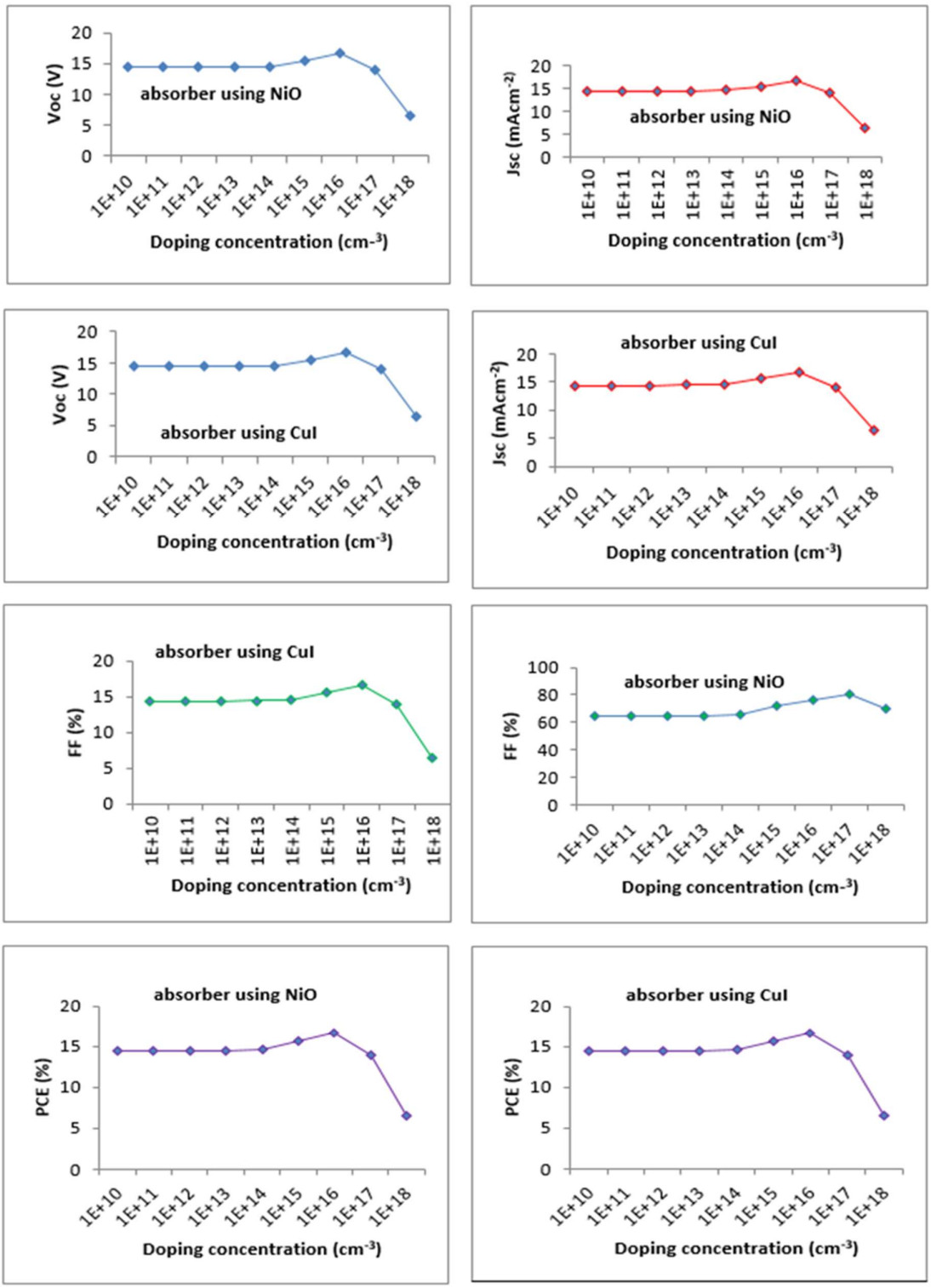

Fig. 8 Variations in performance parameters of PSC with doping concentration of absorber layer with NiO and CuI as HTM

Table V Dependence of solar cell performance on the defect density of Absorber

Parameter N_A (cm^{-3})	V_{oc} (V) NiO	V_{oc} (V) CuI	J_{sc} ($mAcm^{-2}$) NiO	J_{sc} ($mAcm^{-2}$) CuI	FF (%) NiO	FF (%) CuI	PCE (%) NiO	PCE (%) CuI
1E+10	0.93	0.93	21.76	22.06	64.67	70.45	13.07	14.42
1E+11	0.93	0.93	21.76	22.06	64.67	70.45	13.07	14.42
1E+12	0.93	0.93	21.76	22.06	64.68	70.46	13.08	14.42
1E+13	0.93	0.93	21.76	22.06	64.77	70.53	13.09	14.43
1E+14	0.93	0.93	21.80	22.10	65.67	71.25	13.26	14.57
1E+15	0.91	0.91	22.08	22.35	71.66	76.41	14.38	15.56
1E+16	0.87	0.87	21.58	23.08	76.18	82.54	14.23	16.59
1E+17	0.79	0.80	19.17	21.35	79.99	81.52	12.38	13.94
1E+18	0.50	0.50	17.93	18.39	70.05	70.15	6.28	6.47

F. Influence of thickness of ZnO

The effect of the Zinc oxide on the performance parameters of the cell was varied from $0.01\ \mu m$ to $0.07 \mu m$. Fig.9 (a-d) shows the *J-V* curves and QE curves of the simulation with different thickness based on NiO and CuI. Fig.10 (a-d) shows the correlation between the performance parameters and the ZnO thickness. Table VI also shows that when the thickness of the ZnO increases, the value of J_{sc}, FF and PCE of the devices decreases while V_{oc} decreases but remain unchanged from 0.9290 V at the thickness of 0.04 µm for NiO and 0.9272 V at the thickness of 0.03 µm for CuI as HTM. This indicates that when the material is thicker, it provides a longer diffusion path for electron to reach the electrode which limit the charge collection efficiency and transmitting of incident photon decreases with increasing thickness. Optimum value of the cell was obtained when the thickness was $0.01 \mu m$ for both devices with NiO and CuI with V_{oc} of $0.94\ V$, Jsc of $21.83\ mA/cm^2$, FF of 64.82% and PCE of 13.23% for NiO as buffer and V_{oc} of $0.93\ V$, J_{sc} of $22.13\ mA/cm^2$, FF of 70.61% and PCE of 14.59% for CuI as buffer.

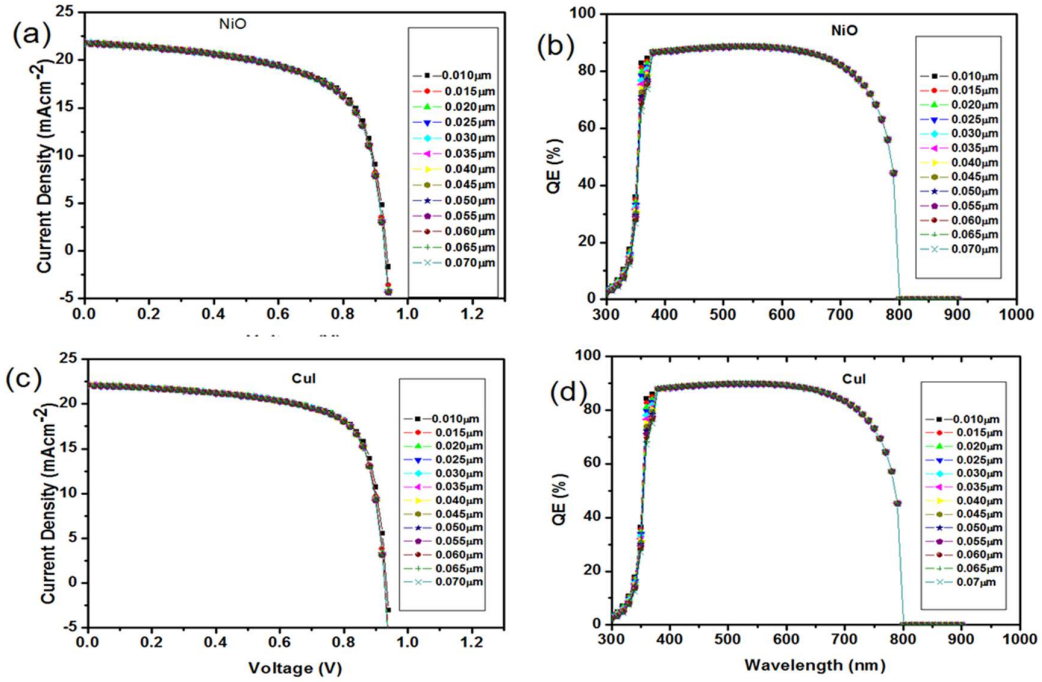

Fig. 9 (a-d) *J–V* curves and QE of PSC with different values of thickness of buffer of NiO and CuI

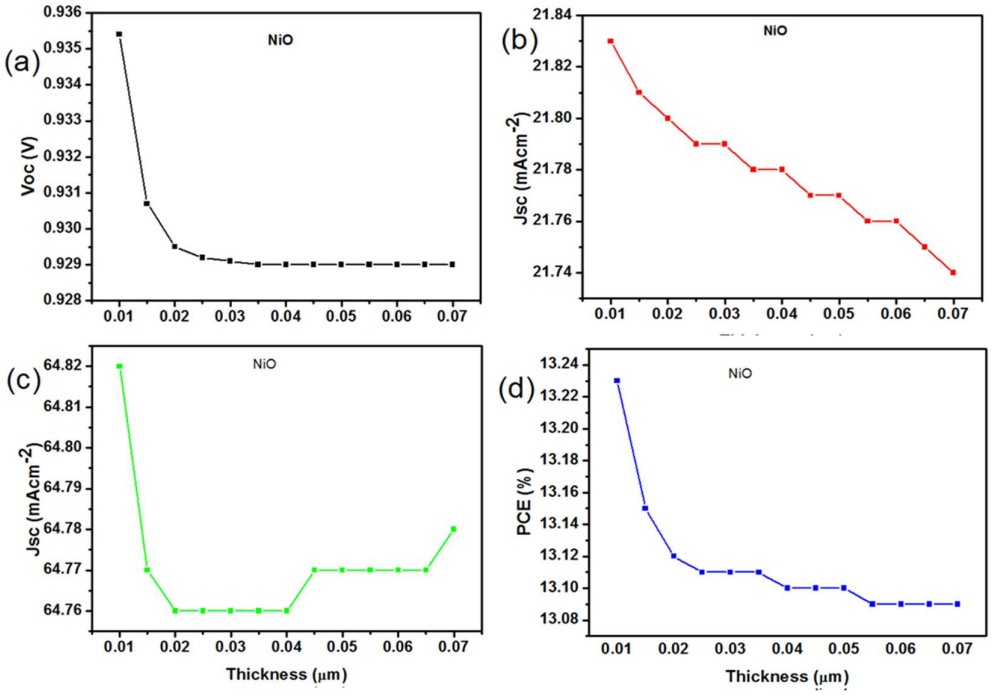

Fig. 10 (a-d) Variation in Performance of PSC with thickness of ETM (ZnO) of NiO

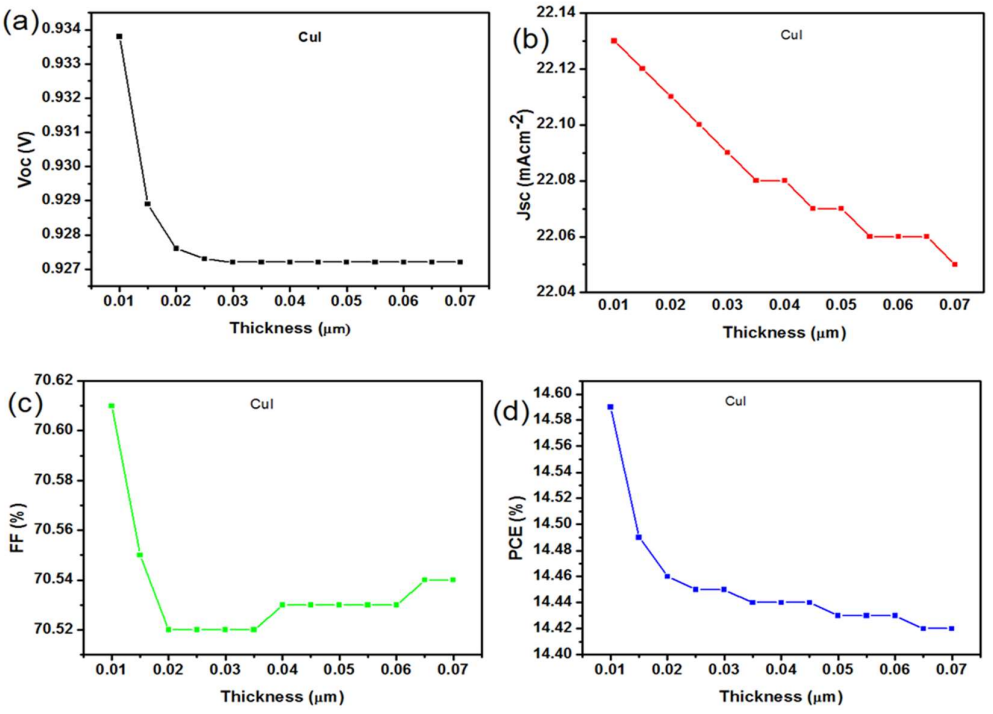

Fig. 11 (a-d) Variation in Performance of PSC with thickness of ETM (ZnO) of CuI

Table VI Dependence of solar cell performance on the thickness of HTM

Parameter T (μ m)	V_{oc} (V) NiO	V_{oc} (V) CuI	J_{sc} (mAcm^{-2}) NiO	J_{sc} (mAcm^{-2}) CuI	FF (%) NiO	FF (%) CuI	PCE (%) NiO	PCE (%) CuI
0.010	0.9354	0.9338	21.83	22.13	64.82	70.61	13.23	14.59
0.015	0.9307	0.9289	21.81	22.12	64.77	70.55	13.15	14.49
0.020	0.9295	0.9276	21.80	22.11	64.76	70.52	13.12	14.46
0.025	0.9292	0.9273	21.79	22.10	64.76	70.52	13.11	14.45
0.030	0.9291	0.9272	21.79	22.09	64.76	70.52	13.11	14.45
0.035	0.9290	0.9272	21.78	22.08	64.76	70.52	13.11	14.44
0.040	0.9290	0.9272	21.78	22.08	64.76	70.53	13.10	14.44
0.045	0.9290	0.9272	21.77	22.07	64.77	70.53	13.10	14.44
0.050	0.9290	0.9272	21.77	22.07	64.77	70.53	13.10	14.43
0.055	0.9290	0.9272	21.76	22.06	64.77	70.53	13.09	14.43
0.060	0.9290	0.9272	21.76	22.06	64.77	70.53	13.09	14.43
0.065	0.9290	0.9272	21.75	22.06	64.77	70.54	13.09	14.42
0.070	0.9290	0.9272	21.74	22.05	64.78	70.54	13.09	14.42

G. Performance of PSC with Optimized parameters

Because The thickness of the absorber, bandgap of the absorber, doping concentration of absorber and defect density of the absorber were optimized for both HTM and the values are as shown in Table VII. The final optimized PSC gave a PCE of 15.74%, J_{sc} of 27.22 mA/cm^2 , V_{oc} of 0.77 V and FF of 74.69% for NiO and PCE of 16.65%, J_{sc} of 24.33 mA/cm^2 , V_{oc} of 0.83 V and FF of 82.43 % for CuI. When the optimized result is compared with the reference initial device, there is an overall improvement in the cell over the device that was not optimized. Fig. 12 shows the *J-V* and QE curves of the optimized devices and Tables VIII and IX compared other results with our simulated results.

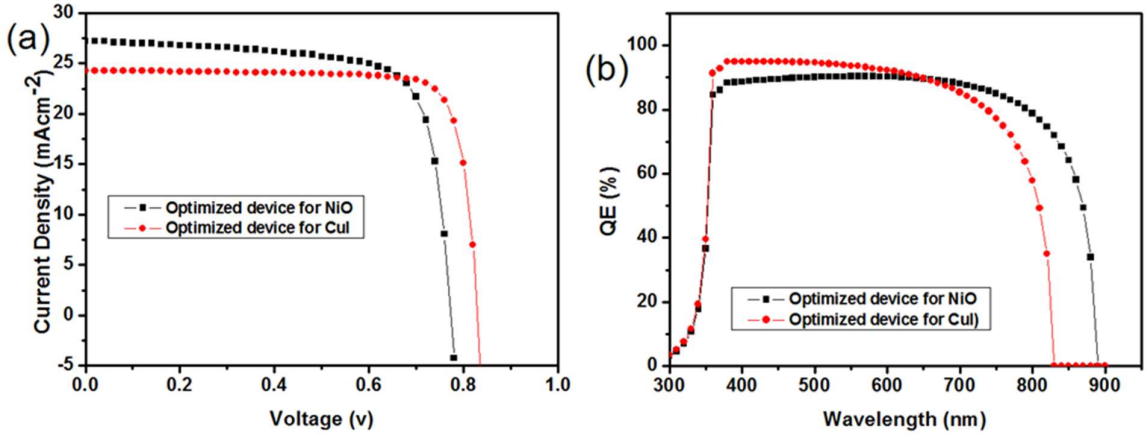

Fig. 12 (a) *J–V* curves of PSC with Optimized parameters, (b) QE of the optimize parameters with respect to wavelength

Table VII Optimized Parameters of the device

Optimized parameters	Absorber ($CH_3NH_3PbI_3$) NiO	CuI
Thickness (μm)	0.45	0.40
Doping density (N_A)(cm^{-3})	1E+15	1E+16
Bandgap (eV)	1.4	1.5
Defect density (Nt) (cm^{-3})	1E+13	1E+13

Table VIII Photovoltaic parameters of HTM (NiO) perovskite solar cells reported in the experimental work in the literature and simulated results using SCAPS [29].

Simulation	J_{sc} (mAcm^{-2})	V_{oc} (V)	*FF*	PCE (%)
Initial	22.76	0.93	64.77	13.09
Optimized N_A of absorber	2.08	0.91	71.66	14.38
Optimized thickness of absorber	21.76	0.93	64.77	13.09
Optimized Bandgap of absorber	26.58	0.78	68.09	14.18
Optimized defect density of absorber	21.76	0.93	64.77	13.09
Final Optimization	27.22	0.77	74.69	15.74
	14.90	0.94	75.00	7.26

Table IX Photovoltaic parameters of HTM (CuI) perovskite solar cells reported in the experimental work in the literature and simulated results using SCAPS [30].

Simulation	J_{sc} (mAcm^{-2})	V_{oc} (V)	*FF*	PCE (%)
Initial	22.07	0.92	70.53	14.43
Optimized N_A of absorber	23.08	0.87	82.54	16.59
Optimized thickness of absorber	21.73	0.92	71.98	14.43
Optimized Bandgap of absorber	23.63	0.88	69.65	14.54
Optimized defect density of absorber	22.07	0.93	70.53	14.43
Final Optimization	24.33	0.83	82.43	16.65
	17.80	0.55	60.00	6.00

IV. CONCLUSION

In this work, the lead-based perovskite solar cells with two different organic HTM i.e. NiO and CuI were analyzed with one-dimensional device simulation. The effect of absorber parameters on the device were analyzed with result indicating an optimum thickness of 0.45 µm for NiO and 0.40 µm for CuI, doping concentration values of 1×10^{15} cm^{-3} and for NiO and 1×10^{16} cm^{-3} for CuI, 1.4 µm for NiO and 1.5 µm for CuI optimum value of bandgap of the absorber and 1×10^{13} cm^{-3} for both NiO and CuI are required for preparing efficient solar cells. From the two HTMs employed, the result shows that CuI as a HTM can achieve relatively higher efficiency which is due to its high mobility, good chemical stability and better chemical iteration with perovskite absorber. This indicates the PCE of the device can further be increase when appropriate parameters are carefully analyzed from the absorber which plays an important role in the PCE enhancement of the devices. Encouraging result with PCE of 16.65 %, FF of 82.54%, J_{sc} of 24.33 mA/cm^2 and V_{oc} of 0.83 V were obtained for CuI as HTM and PCE of 15.74%, FF of 74.69%, J_{sc} of 27.22 mA/cm^2 and V_{oc} of 0.77 *V* were obtained for NiO as HTM which shows an enhancement of ~1.15 times in PCE, ~1.10 in J_{sc} and ~ 1.17 in FF in CuI as HTM and ~1.20 times in PCE, ~1.25 in J_{sc} and ~1.15 in FF for NiO HTM.

ACKNOWLEDGMENT

The authors are grateful to Prof Marc Burgelman and colleagues at the University of Gent for providing the SCAPS-1D software used for this research.

References

[1] A. Kojima, K. Teshima, Y. Shirai and T. Miyasaka, "Organometal halide perovskites as visible-light sensitizers for photovoltaic cells". J. Am. Chem. Soc., vo. 131, pp. 6050–6051, 2009.

[2] M. M. Lee, J. Teuscher, T. Miyasaka, T. N. Murakami, and H. J. Snaith, "Efficient hybrid solar cells based on meso-superstructured organometal halide perovskites". Sci., vol. 338, pp. 643–647, 2012.

[3] M. Liu, M. B. Johnston, and H. J. Snaith, "Efficient planar heterojunction perovskite solar cells by vapour deposition". Nat., vol. 501, pp. 395–398, 2013.

[4] H. Zhou, Q. Chen, G. Li, S. Luo, T-B. Song, H-S. Duan, Z. Hong, J. You, Y. Liu, and Y. Yang, "Interface engineering of highly efficient perovskite solar cells". Sci., vol. 345, pp. 542–546, 2014.

[5] W. S. Yang, J. H. Noh, N. J. Jeon, Y. C. Kim, S. Ryu, J. Seo and S. I. Seok, "High-performance photovoltaic perovskite layers fabricated through intramolecular exchange". Sci., vol. 348, pp. 1234–1237, 2015.

[6] Best research cell efficiencies, NREL, 2016.

[7] H. S. Kim, C. R. Lee, J. H. Im, K. B. Lee, T. Moehl, A. Marchioro, S. J. Moon, R. Humphry- Baker, J. H. Yum, J. E. Moser, M. Grätzel and N. G. Park, "Lead Iodide Perovskite Sensitized All-Solid-State Submicron Thin Film Mesoscopic Solar Cell with Efficiency Exceeding 9%". Sci. Rep., vol. 2, pp. 591, 2012.

[8] J. M. Ball, M. M. Lee, A. Hey, and H. J. Snaith, "Low-temperature processed meso-superstructured to thin-film perovskite solar cells". Energy Environ. Sci., vol. 6, pp. 1739-1743, 2013.

[9] G. A. Casas, M. A. Cappelletti, A. P. Cedola, B. M. Soucase, and E. L. Peltzer, "Analysis of the Power Conversion Efficiency of Perovskite Solar Cells with Different Materials as Hole-Transport Layer by Numerical Simulations". Superlattices Microstruct., vol. 107, pp. 136-143, 2017.

[10] S. Z. Haider, H. Anwar, and M. Q. Wang, "A Comprehensive Device Modelling of Perovskite Solar Cell with Inorganic Copper Iodide as Hole Transport Material". Semicond. Sci. Technol., vol. 33, 2018. Article ID: 035001.

[11] Z. Qu, F. Ma, Y. Zhao, X. Chu, S. Yu and J. You, "Updated Progresses in Perovskite Solar Cells". Chin. Phys. Lett., vol. 38, pp. 107801, 2021.

[12] E. Danladi, M. Kashif, A. Ichoja, and B. B. Ayiya, "Modeling of a Sn-Based HTM-Free Perovskite Solar Cell Using a One-Dimensional Solar Cell Capacitance Simulator Tool". Trans. Tianjin Univ., vol. 28, no. 5, 2022.

[13] A. Yella, L. P. Heiniger, P. Gao, M. K. Nazeeruddin and M. Grätzel, "Nanocrystalline Rutile Electron Layer Enables Low-Temperature Solution-Processed Perovskite Photovoltaics with 13.7% Efficiency". Nano Lett., vol. 14, pp. 2591-2596, 2014.

[14] A. Baktash, O. Amiri and A. Sasani, "Improve the efficiency of Perovskite Solar Cells by using Magnesium Doped ZnO and TiO_2 Compact Layers". Superlattices Microstruct., Vol. 93, pp. 128-137, 2016.

[15] M. Saliba, T. Matsui, K. Domanski, J. Y. Seo, A. Ummadisingu, S. M. Zakeeruddin, J. P. Correa-Baena, W. R. Tress, A. Abate, A. Hagfeldt and M. Gratzel, "Cesium-containing triple cation perovskite solar cells: improved stability, reproducibility, and

high efficiency". Energy Environ. Sci., vol. 9, pp. 1989-1997, 2016.
[16] W. H. Nguyen, C. D. Bailie, E. L. Unger, M. D. McGehee, "Enhancing the hole- conductivity of spiro-OMeTAD without Oxygen". J. of Am. Chem. Soc., vol. 136, pp. 10996-11001, 2014.
[17] A. Intaniwet, C. A. Mills, P. J. Sellin, M. Shkunov, and J. L. Keddie, "Achieving a Stable Time Response in Polymeric Radiation Sensors under Charge Injection by X-Rays". ACS Appl. Mat. Interfaces, vol. 2, pp. 1692-1699, 2010.
[18] E. Danladi, A. Shuaibu, M. S. Ahmad and J. Tasiu, "Numerical modeling and analysis of HTM-free heterojunction solar cell using SCAPS-1D". East Euro. J. Phys., vol. 2021, no. 2, pp. 135-145, 2021.
[19] E. Danladi, A. O. Salawu, M. O. Abdulmalik, E. D. Onoja, E. E. Onwoke, and D. S. Adepehin, "Optimization of Absorber and ETM Layer Thickness for Enhanced Tin based Perovskite Solar Cell Performance using SCAPS-1D Software". Phys. Access, Vol. 2, pp. 1-11, 2022.
[20] R. Wei, "Modelling of Perovskite Solar Cells". M.Sc. Degree Thesis, Queensland Univ. Tech. Queensland city, Australia, 2018.
[21] M. I. Hossain, F. H. Alharbi, and N. Tabet, "Copper oxide as inorganic hole transport material for lead halide perovskite-based solar cells". Sol. Energy, vol. 120, pp. 370-380, 2015.
[22] D. Yang, Z. Yang, W. Qin, Y. Zhang, S. Liu and C. Li, "Alternating precursor layer deposition for highly stable perovskite films towards efficient solar cells using vacuum deposition". J. Mater. Chem. A, vol. 3, pp. 9401-9405, 2015.
[23] D. Chen., Wang, Y., Lin, Z., Huang, J., Chen, X.Z., Pan, D., Huang. F., 2010. "Growth strategy and physical properties of the high mobility of P-types CuI Crystal. Cryst. Growth Des. 10(5), 2057-2060.
[24] F. Kurnia, H. C. U. Jung, C. Liu, S. B. Lee, S. M. Yang, H. W. Park, S. J. Song and C. S. Hwang, "Effect of NiO growth conditions on the bipolar resistance memory switching of Pt/NiO/SRO structure". J. of Korean Phys. Soc., vol. 57, pp. 1856-1861, 2010.
[25] W. Yu, F. Li, H. Wang, E. Alarousu, Y. Chen, B. Lin, L. Wang, M. N. Hedhili, Y. Li, K. Wu, X. Wang, O. F. Mohammed and T. Wu, "Ultrathin Cu_2O as an efficient inorganic hole transporting material for perovskite solar cells". Nanoscale, vol. 8, pp. 6173, 2016.
[26] E. Danladi, M. Y. Onimisi, S. Garba, R. U. Ugbe, J. A. Owolabi, O. O. Ige, G. J. Ibeh and A. O. Muhammed, "Simulation and optimization of lead-based perovskite solar cells with cuprous oxide as a p-type inorganic layer". J. Nig. Soc. Phy. Sci., vol. 1, pp. 72-81, 2019.
[27] A. Amin and M. F. Faruk, "Numerical simulation for the high efficiency p-n Si solar cell with HT-EBL and ET-HBL". 2nd Inter. Conf. on Elect., Comp. & Telecom. Eng. (ICECTE), 8-10 December 2016, Rajshahi-6204, Bangladesh.
[28] U. Mandadapu, S. V. Vedanayakam, and K. Thyagarajan, "Simulation and Analysis of Lead-Based Perovskite Solar Cell Using SCAPS-1D. Indian J. Sci. and Technol., vol. 10, pp. 1-8, 2017.
[29] A. S. Subbin, A. Haider, S. Ghosh, N. Hodes and S. K. Sarkar, "Inorganic hole conducting layers for perovskite-based solar cells". J. Phys. Chem. Lett., vol. 5, pp. 1748-1753, 2014.
[30] A. Christians, R. C. Fung and P. V. Kamat, "An Inorganic Hole Conductor for Organo-Lead Halide Perovskite Solar Cells. Improved Hole Conductivity with Copper Iodide". J. Am. Chem. Soc., vol. 136, no. 2, pp. 758–764, 2014.